Critical Assessment

Diffusion-controlled growth of ferrite plates in plain-carbon steels

The implementation of the theory of diffusion-controlled growth of ferrite plates in plain-carbon steels is critically assessed. It is found that the use of empirically extrapolated diffusion coefficients, phase boundaries, and thermodynamic functions leads to errors in calculations of growth rate. The errors become most important for low transformation temperatures, leading to exaggerated growth rates. Ways of avoiding these difficulties are suggested, and a new analysis of experimental data indicates that the lengthening of Widmanstätten ferrite plates in Fe–C alloys occurs at a rate which is influenced by the diffusion of carbon in the austenite ahead of the interface, assuming that the plates adopt a tip radius consistent with the maximum growth velocity. However, there is a systematic discrepancy between theory and experiment: plate-growth theory seems to underestimate the lengthening rate by some 5 μm s⁻¹. This may have something to do with the lath shape of Widmanstätten ferrite, but an analysis using needle-growth theory does not resolve the problem for data obtained at low lengthening rates. In general, plate-growth theory gives a better explanation of experimental data. The growth of bainite sheaves occurs at a rate much faster than expected from carbon diffusion-controlled growth. If the maximum-velocity hypothesis is incorrect (as it is for dendritic solidification), the above-mentioned discrepancies would be larger.

MST/192

H. K. D. H. Bhadeshia

© 1985 The Institute of Metals. Manuscript received 6 December 1984; in final form 1 April 1985. The author is in the Department of Metallurgy and Materials Science, University of Cambridge.

List of symbols

a, b, c, d — adjustable constants in equation (11)
B_s — bainite start temperature
C_p^α — specific heat capacity of α at constant pressure
$C_p^{\alpha\mu}$ — magnetic component of specific heat capacity of α
C_p^γ — specific heat capacity of γ at constant pressure
$C_p^{\gamma\mu}$ — magnetic component of specific heat capacity of γ
C_V — Debye specific heat capacity of γ
ΔC_{nm} — non-magnetic part of difference in specific heat capacity
D — diffusion coefficient of carbon in γ
D' — that part of D which depends only on T
$\bar{D}$ — weighted average diffusivity
e^γ — electronic specific heat coefficient of γ
E_1 — exponential integral function in equation (21)
ΔE — energy gap
f — activity coefficient of carbon in γ
f_1 — defined by equation (1)
ΔF — activation free energy
g — function of f_1, $g\{f_1\} = r/r_c$
g_0/g_1 — degeneracy ratio
$G^{m\alpha}$ — α-phase magnetic contribution to Gibbs free energy change
$\Delta G_0^{\alpha\gamma}$ — Gibbs free energy change accompanying $\alpha \to \gamma$ transformation in pure iron
$\Delta G_0^{\gamma\alpha}$ — Gibbs free energy change accompanying $\gamma \to \alpha$ transformation in pure iron
h — Planck constant
$H_0^{\alpha\mu}$ — magnetic component of enthalpy of α
$H_0^{\gamma\mu}$ — magnetic component of enthalpy of γ
$\Delta\bar{H}_\gamma$ — partial molar enthalpy of solution of carbon in γ
$\Delta H_0^{\alpha\gamma}$ — enthalpy change for $\alpha \to \gamma$ transformation in pure iron
$\Delta H_0^{\gamma\alpha}$ — enthalpy change for $\gamma \to \alpha$ transformation in pure iron
k — Boltzmann constant
l — length of plate
M^{-1} — average cooling rate from T_i to M_s
M_s — Martensite start temperature
p — Péclet number (dimensionless velocity)
r — radius of plate tip
r_c — critical plate-tip radius at which growth ceases
R — universal gas constant
S_1, S_2, S_3 — functions of Péclet number
ΔS_γ^{xs} — excess partial molar entropy of solution of carbon in γ
t — time
t_1 — time at temperature T_i
T — absolute temperature
T_i — isothermal transformation temperature
v — lengthening rate
V_m — molar volume of ferrite
x — mole fraction of carbon in γ
$\bar{x}$ — mole fraction of carbon in undisturbed γ
x_r — mole fraction of carbon in γ at plate tip
$x^{\alpha\gamma}$ — equilibrium mole fraction of carbon of α at T
$x^{\gamma\alpha}$ — equilibrium mole fraction of carbon of γ at T
γ_m — activity coefficient of activated complex
Γ — capillarity constant
ζ — function containing composition dependence of D
Θ^γ — Debye temperature of γ
λ — distance between {002} austenite planes
σ — interface energy per unit area
τ — average incubation time for Widmanstätten ferrite
τ_a — apparent incubation time for Widmanstätten ferrite
ω_γ — carbon–carbon interaction energy in γ

All carbon concentrations x are expressed as mole fractions. Braces are used exclusively to denote functional relations; e.g. in $D\{x\}$, x is the argument of the function D.

Introduction

The edgewise growth of plate-shaped ferrite (α) from austenite (γ) is always accompanied by a change in the

shape of the transformed region.[1-4] This shape change can be described as an invariant-plane strain with a significant shear component;[1,2] it is generally taken to imply a displacive transformation mechanism and the existence of an atomic correspondence between the parent and product phases, at least as far as atoms in substitutional sites are concerned.[5,6] Interstitial atoms, such as carbon, may diffuse during transformation (especially when the ferrite forms at low undercoolings where the partitioning of carbon is a thermodynamic necessity), without affecting the shape change or the displacive character of the transformation.[5] A displacive mechanism also implies the existence of a glissile, semicoherent α/γ interface, so that if carbon is partitioned during growth, the interface motion can be expected to be controlled by the rate of carbon diffusion in the γ ahead of the moving interface, even when the reaction occurs at a low homologous temperature. On the other hand, diffusional transformations occur by the reconstruction of the parent lattice into that of the product. This requires all atoms to diffuse during reaction, so that the transformation becomes interface controlled at low homologous temperatures. The study of plate-lengthening rates can therefore provide information on the mechanism of transformation.

The theory of diffusion-controlled growth is difficult to implement because the necessary data cannot always be ascertained by experiment. These difficulties are discussed after a brief presentation of the theory. The aim of this work is to assess the application of growth-rate theory to the formation of ferrite plates in plain-carbon steels. New calculations, which avoid certain approximations made in previous studies, are also presented and compared with published experimental data. Only with accurately calculated growth rates is it possible to predict the microstructure of, for example, weld deposits in low-alloy steels.

Theory of diffusion-controlled plate growth

Trivedi[7] has obtained a solution to the problem of diffusion-controlled plate growth. Assuming that as it grows a plate retains the shape of a parabolic cylinder, its growth rate v for steady growth (at a temperature T) controlled by the diffusion of carbon in the γ ahead of the interface is obtained by taking the ratio

$$f_1 = (\bar{x} - x^{\gamma\alpha})/(x^{\alpha\gamma} - x^{\gamma\alpha}) \qquad (1)$$

and solving the equation

$$f_1 = (\pi p)^{1/2} \exp\{p\} \operatorname{erfc}\{p^{1/2}\}[1 + (r_c/r)f_1 S_2\{p\}] \qquad (2)$$

In equation (1) the carbon content $\bar{x}$ of the undisturbed γ, well ahead of the crack tip, can be taken as the average carbon content of the alloy if soft-impingement effects are absent. In equation (2) p is a dimensionless velocity, the Péclet number, given by

$$p = vr/2\bar{D} \qquad (3)$$

(The function $S_2\{p\}$ in equation (2) has been evaluated numerically by Trivedi.) As the diffusion coefficient $D\{x, T\}$ depends on the carbon concentration x, which in turn depends on the distance ahead of the plate tip, the diffusivity used in equation (3) is a weighted average:[8]

$$\bar{D} = \int_{x_r}^{\bar{x}} D\{x, T\} \, dx/(\bar{x} - x_r) \qquad (4)$$

The carbon concentration in the γ at the plate tip, x_r, differs from $x^{\gamma\alpha}$ because of the Gibbs–Thompson capillarity effect:[9] for all finite r

$$x_r = x^{\gamma\alpha}[1 + (\Gamma/r)] \qquad (5)$$

where Γ is the capillarity constant given by[9]

$$\Gamma = \frac{\sigma V_m}{RT} \frac{(1 - x^{\gamma\alpha})/(x^{\alpha\gamma} - x^{\gamma\alpha})}{1 + [d(\ln f)/d(\ln x^{\gamma\alpha})]} \qquad (6)$$

Here it is assumed that the composition of the α is not affected by capillarity, since $x^{\alpha\gamma}$ is always very small. Equation (6) is more accurate than the equation used by Hillert[10] since Henry's law does not apply to solid solutions of Fe-C having the concentrations of interest.[11] Note that r_c can be obtained by setting $x_r = \bar{x}$ in equation (5).

As pointed out above, in Trivedi's solution[7] for diffusion-controlled growth the plate is assumed to maintain a constant shape, that of a parabolic cylinder. This is not quite so since the capillarity effect implies that x_r varies over the surface of the parabolic cylinder, and this should lead to a deviation from the parabolic shape. Trivedi claims that the variation in x_r has a negligible effect provided the tip radius is greater than $3r_c$.
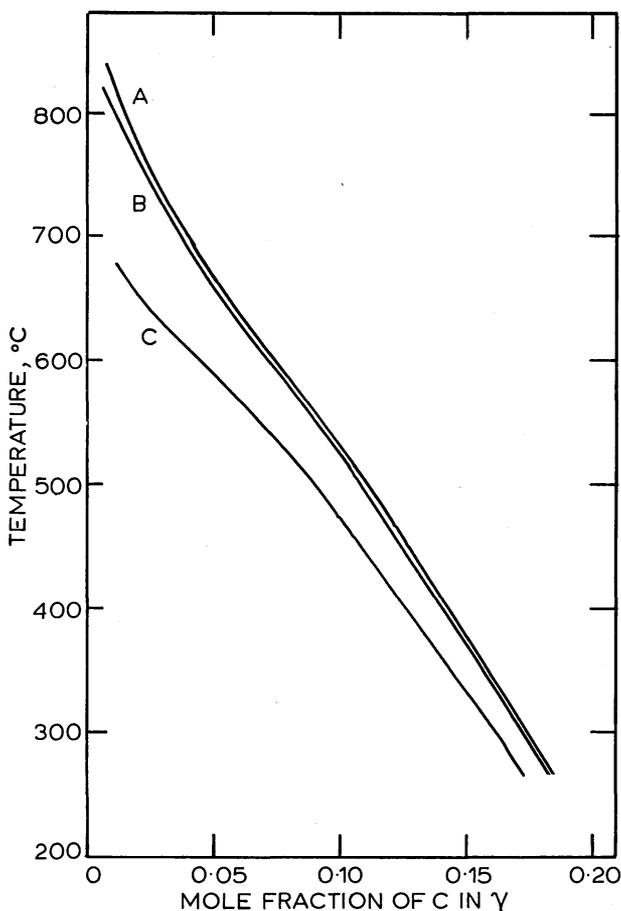
Trivedi[7] has also devised a slightly more elaborate theory to take account of any free energy dissipated in interface processes. In this theory, a second function $S_1\{p\}$ is introduced to allow for the variation in this dissipation with the changing orientation of the interface. This refinement is not considered in the present paper because, as is shown below, almost all the growth rates measured experimentally turn out to be higher than expected from the theory of diffusion-controlled growth. If any appreciable part of the driving force is dissipated in interface processes, this discrepancy between experiment and theory can only increase.

Application of plate-growth theory

The approximations often made in applying the plate-growth theory are discussed below. Some improvements are suggested and their implications on growth-rate calculations are presented in the section 'Results and discussion'.

EXTRAPOLATION OF PHASE BOUNDARIES
Experimental data for $x^{\alpha\gamma}$ and $x^{\gamma\alpha}$ have been obtained for Fe-C at temperatures above the eutectoid temperature, but both Widmanstätten ferrite and bainite can form at much lower temperatures. The $\alpha/(\alpha+\gamma)$ and $\gamma/(\gamma+\alpha)$ phase boundaries therefore have to be extrapolated to the temperatures of interest; for $\bar{x}$ greater than about 0·0015, errors in $x^{\alpha\gamma}$ (which is always less than 0·0015) do not significantly affect the growth-rate calculations, although v is sensitive to $x^{\gamma\alpha}$. Hillert [10,12] uses an empirical linear extrapolation of the $\gamma/(\gamma+\alpha)$ phase boundary which leads to an overestimation of $x^{\gamma\alpha}$ compared with extrapolations based on thermodynamic models[11,13-17] of the Fe-C solid solution. All such thermodynamic models give good agreement with available experimental results, but the extrapolations vary considerably in the region below the eutectoid temperature, where the necessary experimental data appear to be inaccessible. The thermodynamic models are of two kinds: regular-solution models and quasi-chemical models. The former usually assume an ideal configurational entropy of solution, even though the Fe-C solution is not random. Many of these regular-solution models also represent thermodynamic functions with empirical polynomials which cannot be extrapolated with confidence. Quasichemical models,[11,13,14] on the other hand, take much better account of the configurational-entropy terms. These models have been discussed elsewhere;[11,15,16] suffice it to say here that the first-order

1 Curves A, B, and C represent $\gamma/(\gamma+\alpha)$ phase boundaries, calculated using Lacher–Fowler–Guggenheim model, assuming stored energy of ferrite to be 0, 50, and 400 J mol^{-1}, respectively

Table 1 Correction of $\Delta G_0^{\alpha\gamma}$ data to allow for nonlinear dependence of C_p^γ on T

T, K	$\Delta G_0^{\alpha\gamma}$, J mol^{-1} (data from Ref. 20)	$\Delta G_0^{\alpha\gamma}$, J mol^{-1} (allowing for $C_p^{\gamma\mu}$)	C_p^γ, J mol^{-1} K^{-1} (corrected)
500	3641·8	3529·2	29·55
600	2834·2	2769·8	29·98
700	2079·5	2046·0	30·55
800	1393·1	1375·7	31·22
900	799·4	793·7	31·94
1000	338·1	336·0	32·69

$\Delta G_0^{\alpha\gamma}\{500 \text{ K}\}$ as deduced by Orr and Chipman exceeds that obtained by Kaufman et al. by 508 J mol^{-1}.

Agren's analysis accurately reproduces the equilibrium part of the Fe–C phase diagram, but in it the enthalpy change for the $\alpha \to \gamma$ transformation in pure iron at 1185 K, $\Delta H_0^{\alpha\gamma}\{1185 \text{ K}\}$, is taken to be 1011 J mol^{-1}, as against the value $899\cdot6 \pm 41\cdot8$ J mol^{-1} calculated from experimental data.[23]

In most calculations[17,20,22] there is assumed to be a linear relation between C_p^γ (the specific heat capacity of γ at constant pressure) and T, and this is consistent with experimental data[20] for $T > 1185$ K. It has been shown[19,24] that the atoms in the γ phase exist in two electronic states, separated by an energy gap ΔE. The ground state is ferromagnetic, and the higher-energy antiferromagnetic state has a higher magnetic moment. This model has been successfully used to rationalize many physical and thermodynamic properties of austenite over a wide range of temperatures, pressures, and alloy contents.[19,21,25–27] The model implies that there is a magnetic component of the specific heat capacity of γ, $C_p^{\gamma\mu}$, given by[19]

$$C_p^{\gamma\mu} = \frac{R(\Delta E/RT)^2(g_0/g_1)\exp\{\Delta E/RT\}}{[(g_0/g_1)\exp\{\Delta E/RT\}+1]^2} \quad \ldots \quad (7)$$

so that $C_p^{\gamma\mu}$ does not vary linearly with T. Kaufman et al.[19] have shown that the degeneracy ratio g_0/g_1 has the value 0·559, and $\Delta E = 3430\cdot9$ J mol^{-1}. In this representation the heat capacity C_p^γ of austenite is given by

$$C_p^\gamma\{T\} = C_V\{\Theta^\gamma/T\}(1+10^{-4}T)+e^\gamma T+C_p^{\gamma\mu}\{T\} \quad (8)$$

$C_p^{\gamma\mu}$ is negligibly small for $T > 1100$ K, and for 1185 K $< T < 1665$ K, C_p^γ is (within experimental error) a linear function of T, given by[20]

$$C_p^\gamma = 23\cdot9743 + 0\cdot0084T \text{ J mol}^{-1}\text{ K}^{-1} \quad \ldots \quad (9)$$

Extrapolation of equation (9) to low temperatures is clearly not justifiable since $C_p^{\gamma\mu}$ becomes significant, especially as compared with $C_p^\gamma - C_p^\alpha$. If $C_p^{\gamma\mu}$ is neglected for $T > 1185$ K but is added to equation (9) for $T < 1185$ K, then the data obtained by Orr and Chipman[20] can be corrected, as in Table 1. The method used for these calculations is otherwise identical to that used by Orr and Chipman. Taking $C_p^{\gamma\mu}$ into account therefore brings a better agreement with the results found by Kaufman et al.,[19] although the differences are still substantial (395 J mol^{-1} at 500 K). Neither Agren[17] nor Hillert and Jarl[22] considered $C_p^{\gamma\mu}$, and they all assumed C_p^γ to be a linear function of T.

The Debye temperatures and the electronic specific-heat coefficients for γ and α are virtually identical.[19] This means that $C_p^\gamma - C_p^\alpha = C_p^{\gamma\mu} - C_p^{\alpha\mu}$, so there is no difference in the nonmagnetic part of the specific heat capacities of each phase. It follows that the enthalpy change for the $\alpha \to \gamma$ transformation in pure iron is given by

$$\Delta H_0^{\alpha\gamma}\{T\} = \Delta H_0^{\alpha\gamma}\{0 \text{ K}\} + H_0^{\gamma\mu}\{T\} - H_0^{\alpha\mu}\{T\} \quad \ldots \quad (10)$$

Kaufman et al.[19] found that with $\Delta H_0^\alpha\{0 \text{ K}\} = 5452$ J mol^{-1}, a value $\Delta H_0^{\gamma\alpha}\{1185\} = 879$ J mol^{-1} is obtained,

quasichemical model proposed by McLellan and Dunn[11] is accepted to be the best representation of the Fe–C solid solution. It has been found[15] that values of $x^{\gamma\alpha}$ calculated using this model are identical to those obtained using the Lacher–Fowler–Guggenheim model[13–15] (another quasichemical model, first applied to steels by Aaronson et al.[18] and later corrected by Shiflet et al.[15]). Furthermore, the two models give the same result for the activity of carbon in γ (Ref. 15), so it makes no difference which model is used to analyse plate growth. The present calculations are based on values of $x^{\gamma\alpha}$ (Fig. 1), $x^{\alpha\gamma}$, and f obtained using the Lacher–Fowler–Guggenheim model. The parameters used in applying this model are[15] the carbon–carbon interaction energy in γ, $\omega_\gamma = 8054$ J mol^{-1}; the partial molar enthalpy of solution of carbon in γ, $\Delta \bar{H}_\gamma = 38\,565$ J mol^{-1}; and the excess partial molar entropy of solution of carbon in γ, $\Delta S_\gamma^{xs} = 13\cdot48$ J mol^{-1} K^{-1}.

THERMODYNAMIC FUNCTIONS OF IRON

To calculate $x^{\gamma\alpha}$ requires a knowledge of the change in Gibbs free energy accompanying the $\gamma \to \alpha$ transformation in pure iron, $\Delta G_0^{\gamma\alpha}\{T\}$. Values of $\Delta G_0^{\gamma\alpha}\{T\}$ have been deduced by several investigators,[17,19–22] but these values differ significantly at temperatures below about 1000 K. The differences at low temperature cannot be attributed simply to the use of different experimental data, but arise largely because the properties of metastable phases are sometimes extrapolated empirically. For $T < 1000$ K, Hillert and Jarl[22] obtained results similar to those found by Kaufman et al.,[19] but different from those found by Orr and Chipman,[20] and by Agren.[17] The value of

which compares well with the selected experimental value $\Delta H_0^{\gamma\alpha}\{1185\} = 899{\cdot}6$ J mol^{-1} (Ref. 23). Orr and Chipman[20] also use $\Delta H_0^{\gamma\alpha}\{1185\} = 899{\cdot}6$ J mol^{-1} in their analysis, but because their value for $\Delta H_0^{\gamma\alpha}\{0$ K$\}$ is much greater than 5452 J mol^{-1}, their results are in this sense internally inconsistent, as are Agren's[17] (applying equation (10) gives a value of $\Delta H_0^{\gamma\alpha}\{1185\}$ different from the assumed values).

Hillert and Jarl[22] and Agren[17] use a polynomial equation to represent $\Delta G_0^{\alpha\gamma}$:

$$\Delta G_0^{\alpha\gamma} = a + bT + cT \ln T + dT^2 + G^{m\alpha} \quad . \quad . \quad . \quad (11)$$

where a, b, c and d are four adjustable constants obtained by fitting equation (11) to four experimental data. The shortcomings of this technique are emphasized by the fact that the two analyses[22,17] yield very different values of the four parameters, simply because Agren chose a slightly larger value for $\Delta G_0^{\alpha\gamma}\{1000$ K$\}$. The non-magnetic part of the difference in specific heat capacity, ΔC_{nm}, is assumed to be given by the linear equation (with $C_p^{\gamma\mu} = 0$)

$$\Delta C_{nm} = C_p^{\alpha} - C_p^{\gamma} - C_p^{\alpha\mu} + C_p^{\gamma\mu} = -c - 2dT \quad . \quad . \quad . \quad (12)$$

Both analyses[22,17] yield finite values for c and d, even though ΔC_{nm} should equal zero since the Debye temperatures and electronic specific heat coefficients of α and γ are equal.

The analysis by Kaufman et al.[19] does not suffer from the difficulties discussed above. Their results successfully predict[25,26] the pressure and temperature dependences of the $\gamma \to \alpha$ and $\gamma \to$ hcp iron transformations at pressures up to 160 kbar and temperatures between 300 and 1183 K. Roy and Kaufman[27] also found good agreement between determinations of $\Delta G_0^{\gamma\alpha}$ based on measurements of the activity and specific heat capacity of Fe–Mn alloys, and the results obtained by Kaufman et al., which were based on completely different data. This comparison is particularly relevant because the work of Roy and Kaufman covers temperatures down to 500 K. Kaufman and Nesor[21] have successfully used the thermodynamic data[19] in the calculation of Fe–Ni, Fe–Cr, and Fe–Co phase diagrams.

It appears then, that the results obtained by Kaufman et al.[19] on the change in the Gibbs free energy accompanying transformations in pure iron are well established, reliable, and accurate for low-temperature applications. Hence, unless otherwise specified, these tabulations[19] are used in the calculations below.

EXTRAPOLATION OF DIFFUSION COEFFICIENT

It is necessary to know $D\{x, T\}$, at least over the ranges $x^{\gamma\alpha} > x > \bar{x}$ and 1200 K $> T > 550$ K; experimental determinations of $D\{x, T\}$ do not extend beyond $x > 0{\cdot}06$ and for $T < 1000$ K. Many earlier determinations of plate growth rates[8,28] have been based on the extrapolation of an empirical representation of $D\{x, T\}$ (Ref. 29). A better method, used in the present study, is that used by Siller and McLellan,[30,31] who developed a theoretical model for $D\{x, T\}$ and demonstrated its compatibility with both the kinetic and the thermodynamic behaviour of carbon in austenite. According to this model,

$$D\{x, T\} = D'\zeta\{x\} \quad . \quad . \quad . \quad . \quad . \quad . \quad . \quad . \quad . \quad (13)$$

D' being a function only of T,

$$D' = (kT/h)[\exp(-\Delta F/kT)](\lambda^2/3\gamma_m) \quad . \quad . \quad . \quad . \quad (14)$$

where ΔF is an activation free energy ($\Delta F/k = 21\,230$ K, Ref. 32). The term $\lambda^2/3\gamma_m$ arises from reaction-rate theory, and has been shown to be given by $\ln(3\gamma_m/\lambda^2) = 31{\cdot}84$ (Ref. 32). Note that $\zeta\{x\}$ contains the entire composition dependence of D (for details see Refs. 30–32).

OTHER PARAMETERS

Because the plates all seem to grow by a displacive mechanism, there is always a reproducible orientation
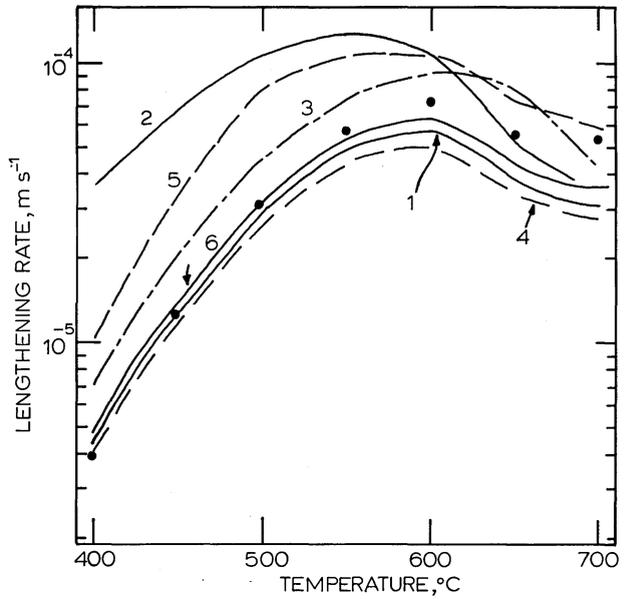
2 **Calculations of lengthening rate v for Fe–0·2 wt-%C, assuming stored energy of Widmanstätten ferrite to be zero; curves (for details *see* text) all represent maximum plate growth rates, while data points represent maximum needle growth rates**

relationship between the α and γ such that the closest-packed planes of the two lattices are nearly parallel, as are the close-packed directions within these planes.[1] This means that the α/γ interface energy σ should be similar to that of martensite/austenite interfaces. Consequently, σ can be taken to be the same for all plates, i.e. $0{\cdot}2$ J m^{-2} (the martensite/γ interface energy[33]) for the interface where growth occurs. If the linear-expansion coefficient of ferrite is taken to be $1{\cdot}2 \times 10^{-5}$ K^{-1} (Ref. 34), and the ambient-temperature α-lattice parameter $0{\cdot}2866$ nm, then the molar volume of ferrite may be written as

$$V_m = [1 + 3{\cdot}6 \times 10^{-5}(T - 298)](7{\cdot}09 \times 10^{-6}) \text{ m}^3 \text{ mol}^{-1} \tag{15}$$

Throughout this work, in all theoretical calculations of v it is assumed that the Zener hypothesis,[35] that the plate adopts a tip radius which allows v to be maximized, can be applied.

Results and discussion

Calculations of v were made for an Fe–0·2 wt-%C alloy; the results (Fig. 2) illustrate the influence of the approximations mentioned above. Curve 1 in Fig. 2 shows the best set of calculations, based on a value of D calculated from equation (13), Γ from equation (6), data for $\Delta G_0^{\alpha\gamma}$ obtained by Kaufman et al.,[19] and $x^{\gamma\alpha}$ and f calculated according to the Lacher–Fowler–Guggenheim model. Unless otherwise specified, the other data in Fig. 2 are calculated as for curve 1. The exaggerated low-temperature growth rates caused by choosing an empirical value of D (Ref. 29) are illustrated by curve 2. A smaller, but similar effect (curve 3) arises if $\Delta G_0^{\alpha\gamma}$ from Orr and Chipman is substituted for that obtained by Kaufman et al. The use of the semi-empirical capillarity constant from Simonen et al. (equation (4) of Ref. 28 – their notation for Γ implies a different sign in our equation (5)) seems to have only a small effect on v (curve 4). Simonen et al.[28] used $x^{\gamma\alpha}$ data from Ref. 18 in their growth-rate calculations; these data were later shown to be incorrect,[15] and the effect of using

them is illustrated in curve 5. They also used the empirical D in their calculations, which results in highly exaggerated results for low temperatures. This explains why they found such great disagreement between experiment and theory for $T < 973$ K. Finally, the lesser effect of letting $x^{\alpha\gamma}$ equal a constant value of 0·03 wt-% is represented by curve 6.

There is an interesting consequence of the Zener maximum-velocity hypothesis, as applied to Trivedi's model for plate growth. Trivedi has shown[7] that for maximum growth rate, the ratio r/r_c is a function g of f_1 so that $r/r_c = g\{f_1\}$ (Fig. 4 of Ref. 7), where r_c is a critical plate-tip radius at which growth ceases (i.e. $x_r = \bar{x}$). From equation (5) it follows that

$$r_c = \Gamma x^{\gamma\alpha}/(\bar{x} - x^{\gamma\alpha}) \qquad \ldots \ldots \ldots \ldots (16)$$

and hence that

$$r = \Gamma x^{\gamma\alpha} g\{f_1\}/(\bar{x} - x^{\gamma\alpha}) \qquad \ldots \ldots \ldots (17)$$

Substitution for r in equation (5) then shows that x_r does not depend on Γ, and hence is not a function of σ when the maximum-velocity criterion is assumed. Nevertheless, σ affects v since

$$v = 2\bar{D}p/r$$
$$= 2\bar{D}p(\bar{x} - x^{\gamma\alpha})/\Gamma x^{\gamma\alpha} g\{f_1\} \qquad \ldots \ldots \ldots (18)$$

Since p depends only on f_1 and r/r_c, it follows (within the context of Zener's hypothesis) that for a constant f_1, v is inversely proportional to σ. Doubling σ halves v, and so the effect of σ on any v data calculated on the basis of the Zener hypothesis is easily deduced.

The displacive formation of Widmanstätten ferrite seems to involve the cooperative growth of mutually accommodating crystallographic variants.[36,37] The resulting surface relief thus consists of two adjacent and opposing invariant-plane strains, so that the elastically accommodated strain energy accompanying plate formation is rather small (of the order of 50 J mol^{-1}). Bainite plates, which grow at higher undercoolings, show surface-relief effects corresponding to single invariant-plane strains, so that the strain-energy term is larger, amounting to about 400 J mol^{-1} (Ref. 36). The effect of these strain-energy terms is to shift the $\gamma/(\gamma + \alpha)$ phase boundary to lower carbon levels (Fig. 1). They are, however, often ignored but, as is shown below, they can have a significant influence on growth rates.

All subsequent calculations are as for curve 1 of Fig. 2.

ANALYSIS OF EXPERIMENTAL DATA

The edgewise growth of ferrite plates in plain-carbon steels has been measured indirectly[12,28,38] by determining the length l of the longest plate observed on a section chosen at random of any given specimen of a series of samples isothermally transformed for various times. Within the limitations of this technique v seems to be constant, even though plates often form in colonies;[38] this could be taken to imply that soft-impingement effects may not be significant.[38] The use of optical microscopy in such experiments limits the resolution of the measurements, and the data for bainite should be taken to represent sheaf growth rates rather than subunit growth rates (the subunit mechanism has been discussed in Refs. 6 and 39). In plain-carbon steels, cementite precipitation rapidly follows the formation of bainitic ferrite, and the effects of carbide precipitation on growth rates cannot be established. These reservations should be borne in mind when considering the data analysed below.

The experimental data used in the analysis are taken from Townsend and Kirkaldy,[38] Hillert,[12] and Simonen et al.;[28] all data are based on the indirect technique discussed above.

The experiments are all concerned with steels which have poor hardenability, and there are indications that some

Table 2 Calculated transformation bainite and martensite start temperatures, °C

$\bar{x}$, wt-%	B_s	M_s
0·235	597	469
0·24	596	467
0·29	582	446
0·33	569	428
0·385	553	404
0·405	545	394
0·43	537	383
0·49	518	355

transformation occurred during the quench from the isothermal transformation temperature, T_i. The formation of Widmanstätten ferrite at any T_i is associated with an average incubation time τ, given by the intercept on the time axis in a plot of l versus t ($t = 0$ when T_i is reached).[38] The τ data must always be positive, but if additional transformation occurs during cooling from T_i to M_s, then the apparent incubation period τ_a can be negative since

$$l = v\{T_i\}(t_1 - \tau) + M \int_{T_i}^{M_s} v\{T\} \, dT \qquad \ldots \ldots (19)$$

where M^{-1} is the average cooling rate from T_i to M_s and t_1 is the time at T_i. It follows that

$$\tau_a = v\{T_i\}\tau - M \int_{T_i}^{M_s} v\{T\} \, dT \qquad \ldots \ldots (20)$$

Figure 1 of Ref. 28 and Fig. 53 of Ref. 40 are both plots of l versus t, for plain-carbon steels, for which τ is negative. In these circumstances the data for absolute length may be unreliable, but equations (19) and (20) show that v derived from dl/dt is unaffected by any spurious transformation during the quench.

The data[12,28,38] cover a range of carbon concentrations from $\bar{x} = 0·0108$ to $0·0229$ and a range of isothermal transformation temperatures from $T = 723$ to 990 K. For data obtained at low temperatures, it is sometimes not clear whether the products examined correspond to bainite or to Widmanstätten ferrite. Bhadeshia[36] has developed thermodynamic criteria which allow these products to be distinguished, given that the formation of Widmanstätten ferrite involves the equilibrium partitioning of carbon during growth, whereas bainite forms with the parent austenite composition. If nucleation is not a limiting factor, Widmanstätten ferrite begins to form when the chemical driving force exceeds 50 J mol^{-1} (the stored energy of Widmanstätten ferrite). Similarly, bainite begins to form when the change in chemical free energy accompanying diffusionless transformation exceeds its stored energy (400 J mol^{-1}). For the plain-carbon steels under consideration, nucleation (as discussed in Ref. 36) is not a limiting factor. Martensite start temperatures can also be calculated thermodynamically;[41] results of calculations of M_s and B_s are given in Table 2.

Figures 3 and 4 show the calculated lengthening rates; the curves B, C, and D refer to the growth of ferrite plates controlled by the diffusion of carbon, the plates having stored energies of 0, 50, and 400 J mol^{-1}, respectively. If the experimental data for Widmanstätten ferrite (circles) are compared with the C curves, all the experimental data, without exception, are seen to exceed the calculated growth rates. This is so (with one exception) also when the data are compared with the B curves. A Widmanstätten ferrite plate is not shaped like a parabolic cylinder, but is lath like;[1] and this may be the reason for the high observed lengthening rate. The curves A in Figs. 3 and 4 represent the carbon diffusion controlled growth of ferrite needles (paraboloids of revolution) with a stored energy of 50 J mol^{-1}. The needle shape is not a valid representation
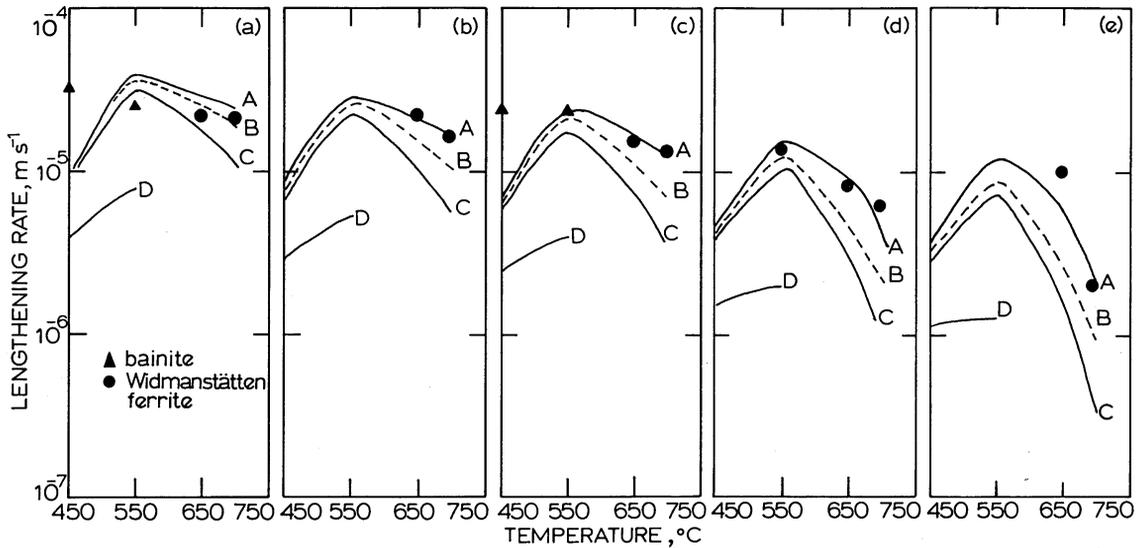
a 0·24C; *b* 0·29C; *c* 0·33C; *d* 0·43C; *e* 0·49C

3 Calculations of (maximum) lengthening rate *v* (curves) compared with experimental data obtained for bainite and Widmanstätten ferrite by Hillert[12] and by Simonen *et al.*[28] (data points) for various carbon contents (wt-%); curves A represent needle lengthening rates, stored energy 50 J mol^{-1}; curves B, C, and D represent plate lengthening rates, stored energies 0, 50, and 400 J mol^{-1}, respectively

of lath-like Widmanstätten ferrite, which has a definite macroscopic invariant plane, but it was felt that the actual value of *v* may fall somewhere between the results for plates and needles.

Figure 5 shows that the plate model consistently underestimates lengthening rates, whereas the needle model underestimates *v* for low f_1 and overestimates *v* for high f_1. The linear-regression correlation coefficients between the experimental and calculated data are 0·73 and 0·87 for the needle and plate models, respectively, and these values are not affected by the choice of σ. On this basis alone, it is tentatively concluded that the plate model gives a better representation of the lengthening of Widmanstätten ferrite; the theoretical underestimation of *v* could have been attributed to the lath-like shape of

Widmanstätten ferrite, but for the fact that the needle model underestimates *v* for low f_1. The reasons for this discrepancy are not clear. The difficulties arise even though the growth rates all refer to the maximum possible *v*, and this suggests that the transfer of atoms across the interface is not rate limiting, even at the lowest of transformation temperatures, which is consistent with the displacive formation of Widmanstätten ferrite.
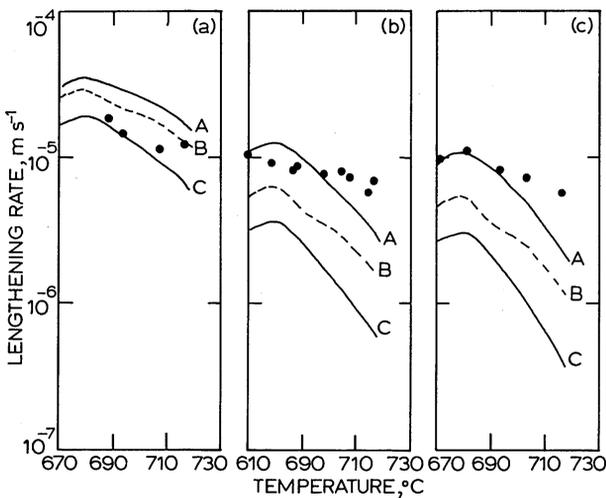
a 0·235C; *b* 0·385C; *c* 0·405C

4 Calculations of lengthening rate *v* (curves) compared with experimental data for Widmanstätten ferrite obtained by Townsend and Kirkaldy[38] (data points) for various carbon contents (wt-%); curves A represent needle lengthening rates, stored energy 50 J mol^{-1}; curves B and C represent plate lengthening rates, stored energies 0 and 50 J mol^{-1}, respectively
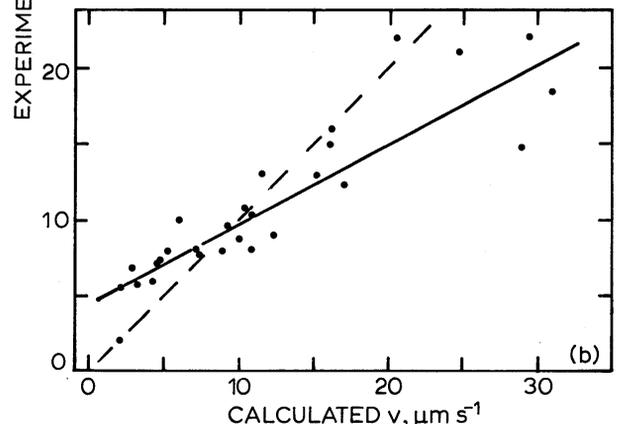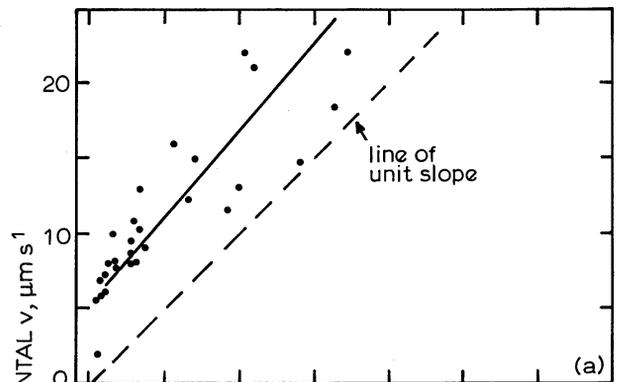
a plates; *b* needles

5 Correlation of experimental and calculated plate and needle lengthening rate *v* for Widmanstätten ferrite

The needle growth rates discussed above were calculated using the equation[7]

$$f_1 = p \exp\{p\}E_1\{p\}[1+(r_c/r)f_1S_3\{p\}] \quad \ldots \quad (21)$$

$S_3\{p\}$ has been evaluated numerically by Trivedi,[7] and r_c is twice as large as it is for plates, making x_r relatively smaller than it is for plates. Trivedi suggested that because $\bar{D}$ increases with x_r, plate growth rates should exceed needle growth rates at a sufficiently low temperature. This effect has been confirmed and is illustrated in Fig. 1, for Fe-0·2 wt-%C, where the points represent needle growth rates. Comparison with curve 1 shows that needle growth rates fall below plate growth rates at a temperature below the M_s temperature.

In the calculations for lengthening rates of needles and plates presented in this paper, Zener's hypothesis – that the tip radii are such that they lead to the maximum v – has been assumed; however, there are no suitable data on plate-tip radii. Simonen *et al.*[28] reported measurements of r, but these were obtained separately from v data, and in any case do not seem to account for stereological effects. Recent work[42-47] on the dendritic growth of solid from liquid (formally an almost identical problem to the present work) has demonstrated conclusively that the dendrites do not attain a radius consistent with the maximum-velocity hypothesis, the actual tip radius being determined by a shape-stability criterion.[45-47] If these results can be extrapolated to solid-state transformations, then the calculated growth velocities would be further reduced, and the discrepancy between experiment and theory would increase, the experimental rates being much higher than those predicted. More work needs to be done on the application of morphological stability theory to solid-state transformations where an invariant-plane-strain shape change accompanies the formation of the product phase. The shape of Widmanstätten ferrite and bainite is determined by the need to minimize the strain energy associated with this shape change, and it is not clear whether shape-stability criteria based on interface stability in diffusion fields are appropriate in these circumstances.

Finally, we note that although 'shape-preserving' solutions have been used in the above calculations, optical microscopy suggests that the shape of Widmanstätten ferrite may not remain constant throughout unhindered growth.[37]

Considering the limited number of data on bainite sheaf lengthening rates in plain-carbon steels, comparison with the D curves in Fig. 3 shows that sheaf growth rates considerably exceed those to be expected when controlled by carbon diffusion, and this is consistent with recent work which suggests that bainitic ferrite grows with a supersaturation of carbon,[6,36] and also with direct observations which show that bainite subunit lengthening rates far exceed those expected if growth were controlled by carbon diffusion.[48] It should be noted that in the Fe-0·24 wt-%C alloy (Fig. 3), one of the bainite points lies below the M_s temperature of the steel.

Conclusions

The application of plate-growth theory to plain-carbon steels has been critically assessed, and the use of empirical representations of diffusion data, thermodynamic functions, and phase boundaries have been found to lead to exaggerated lengthening rates for low temperatures. Refined calculations suggest that Widmanstätten ferrite lengthens at a rate which is faster (generally by a factor of up to 2) than would be expected from the theory of diffusion-controlled plate growth, even though the calculations are based on the assumption of the Zener maximum-

velocity hypothesis. The discrepancy may arise because Widmanstätten ferrite does not grow in the form of plates, but analysis using needle growth theory suggests that the difficulties are not entirely due to the misrepresentation of shape. Plate-growth theory nevertheless correctly predicts the variations in growth rate as a function of temperature and carbon content, and can therefore be used in predicting microstructural variations due to composition and heat treatment. Further work is necessary in determining the accuracy of low-f_1 lengthening-rate data and of plate-tip radii. If plate-tip radii turn out to be different from those consistent with the Zener maximum-velocity hypothesis, the discrepancy noted above will be greater, the actual growth rates considerably exceeding those predicted.

Acknowledgments

References

1. J. D. WATSON and P. G. McDOUGALL: *Acta Metall.*, 1973, **21**, 961–973.
2. G. R. SPEICH: in 'Decomposition of austenite by diffusional processes), (ed. V. F. Zackay and H. I. Aaronson), 353–370; 1962, New York, Interscience.
3. T. KO and S. A. COTTRELL: *J. Iron Steel Inst.*, 1952, **172**, 307–313.
4. T. KO: *J. Iron Steel Inst.*, 1953, **175**, 16–18.
5. J. W. CHRISTIAN: in 'Decomposition of austenite by diffusional processes', (ed. V. F. Zackay and H. I. Aaronson), 353–370; 1962, New York, Interscience.
6. J. W. CHRISTIAN and D. V. EDMONDS: in 'Phase transformations in ferrous alloys', (ed. A. R. Marder and J. I. Goldstein), 293–326; 1983, Warrendale, Pa, The Metallurgical Society of AIME.
7. R. TRIVEDI: *Metall. Trans.*, 1970, **1**, 921–927.
8. R. TRIVEDI and G. M. POUND: *J. Appl. Phys.*, 1967, **38**, 3569–3576.
9. J. W. CHRISTIAN: 'Theory of transformations in metals and alloys', 2 edn, Part 1, 180–181; 1975, Oxford, Pergamon Press.
10. M. HILLERT: *Metall. Trans.*, 1975, **6A**, 5–19.
11. R. B. McLELLAN and W. W. DUNN: *J. Phys. Chem. Solids*, 1969, **30**, 2631–2637.
12. M. HILLERT: 'Growth of ferrite, bainite and martensite', Internal report, Swedish Institute for Metals Research, 1960.
13. J. R. LACHER: *Proc. Camb. Philos. Soc.*, 1937, **33**, 518.
14. R. H. FOWLER and E. A. GUGGENHEIM: 'Statistical thermodynamics'; 1939, New York, Cambridge University Press.
15. G. J. SHIFLET, J. R. BRADLEY, and H. I. AARONSON: *Metall. Trans.*, 1978, **9A**, 999–1007.
16. H. K. D. H. BHADESHIA: *Met. Sci.*, 1982, **16**, 167–169.
17. J. AGREN: *Metall. Trans.*, 1979, **10A**, 1847–1852.
18. H. I. AARONSON, H. A. DOMIAN, and G. M. POUND: *Trans. AIME*, 1966, **236**, 753–767.
19. L. KAUFMAN, E. V. CLOUGHERTY, and R. J. WEISS: *Acta Metall.*, 1963, **11**, 323–335.
20. R. L. ORR and J. CHIPMAN: *Trans. AIME*, 1967, **239**, 630–633.
21. L. KAUFMAN and H. NESOR: *Z. Metallkd.*, 1973, **64**, 249–257.
22. M. HILLERT and M. JARL: *Calphad*, 1978, **2**, 227–238.
23. R. HULTGREN *et al.*: 'Selected values of the thermodynamic properties of elements', 181; 1967, Metals Park, Ohio, American Society for Metals.
24. R. J. WEISS: *Proc. Phys. Soc.*, 1963, **82**, 281.
25. G. STEPAKOFF and L. KAUFMAN: *Acta Metall.*, 1968, **16**, 13–22.
26. L. D. BLACKBURN, L. KAUFMAN, and M. COHEN: *Acta Metall.*, 1965, **13**, 533–541.

27. P. ROY and L. KAUFMAN: *Acta Metall.*, 1965, **13**, 1277–1279.
28. E. P. SIMONEN, H. I. AARONSON, and R. TRIVEDI: *Metall. Trans.*, 1973, **4**, 1239–1245.
29. L. KAUFMAN, S. V. RADCLIFFE, and M. COHEN: in 'Decomposition of austenite by diffusional processes', (ed. V. F. Zackay and H. I. Aaronson), 313–352; 1962, New York, Interscience.
30. R. H. SILLER and R. B. McLELLAN: *Trans. AIME*, 1969, **245**, 697–700.
31. R. H. SILLER and R. B. McLELLAN: *Metall. Trans.*, 1970, **1**, 985–988.
32. H. K. D. H. BHADESHIA: *Met. Sci.*, 1981, **15**, 477–479.
33. J. W. CHRISTIAN: in Proc. Int. Conf. on 'Martensitic transformations', ICOMAT 79, 1979, Cambridge, Mass, 220–238.
34. R. C. WEAST (ed.): 'Handbook of chemistry and physics', 57 edn; 1974, Ohio, CRC Press.
35. J. W. CHRISTIAN: 'Theory of transformations in metals and alloys', 2 edn, Part 1, 495; 1975, Oxford, Pergamon Press.
36. H. K. D. H. BHADESHIA: *Acta Metall.*, 1981, **29**, 1117–1130.
37. H. K. D. H. BHADESHIA: *Scr. Metall.*, 1980, **14**, 821–824.
38. R. D. TOWNSEND and J. S. KIRKALDY: *Trans. ASM*, 1968, **61**, 605–619.
39. H. K. D. H. BHADESHIA and D. V. EDMONDS: *Acta Metall.*, 1980, **28**, 1265–1273.
40. H. I. AARONSON: in 'Decomposition of austenite by diffusional processes', (ed. V. F. Zackay and H. I. Aaronson), 387–548; 1962, New York, Interscience.
41. H. K. D. H. BHADESHIA: *Met. Sci.*, 1981, **15**, 175–177.
42. M. E. GLICKSMAN, R. J. SCHAEFER, and J. D. AYRES: *Metall. Trans.*, 1976, **7A**, 1747–1759.
43. S. C. HUANG and M. E. GLICKSMAN: *Acta Metall.*, 1981, **29**, 701–715.
44. S. C. HUANG and M. E. GLICKSMAN: *Acta Metall.*, 1981, **29**, 717–734.
45. J. S. LANGER and H. MULLER-KRUMBHAAR: *Acta Metall.*, 1978, **26**, 1681–1687.
46. J. S. LANGER and H. MULLER-KRUMBHAAR: *Acta Metall.*, 1978, **26**, 1689–1695.
47. J. S. LANGER and H. MULLER-KRUMBHAAR: *Acta Metall.*, 1978, **26**, 1697–1708.
48. H. K. D. H. BHADESHIA: in 'Phase transformations in ferrous alloys', (ed. A. R. Marder and J. I. Goldstein), 335–340; 1983, Warrendale, Pa, The Metallurgical Society of AIME.

The Charles Hatchett Award

Description of Award

The Award, for travel to Brazil (and possibly for travel to Europe for a prize winner from Latin America) with maintenance for approximately two weeks, is administered by The Institute of Metals and is granted annually from funds provided by the Companhia Brasileira de Metalurgia e Mineração (CBMM) to individuals who, in the judgment of a panel of experts, publish papers of outstanding merit within the following range of subjects:

(i) the extractive metallurgy of niobium
(ii) the physical and applied metallurgy of steels and alloys containing niobium either alone or in combination with other metals
(iii) the fabrication and application of structures and components made from such steels and alloys.

Constitution

An International Consultative Panel of not less than six and not more than eight members, who are required to be individuals of knowledge and standing in the metallurgical science, production, and use of niobium, selects the prize-winning paper.

The Panel is appointed by The Institute of Metals in consultation with CBMM for a period of three years, the Council of the Institute having the right to reappoint members once in consultation with CBMM.

The following are the present members of the Panel:

Prof. T. Araki (Kobe Steel Ltd, Tokyo)
Dr A. C. Gréday (Centre de Recherches Métallurgiques, Liège)
Dr S. R. Keown (Consultant, Sheffield)
Dr P. R. Krahe (Paulo Abib Engenharia S/A, Rio de Janeiro)
Prof. W. S. Owen (Massachusetts Institute of Technology)
Prof. G. Petzow (Max-Planck-Institut für Metallforschung, Stuttgart)
Dr F. B. Pickering (Sheffield City Polytechnic, Sheffield)